

# PHYSICAL REVIEW B

## CONDENSED MATTER

THIRD SERIES, VOLUME 51, NUMBER 18

1 MAY 1995-II

### Nitrogen diffusion and distribution in the $Y_2Fe_{17}$ lattice

Y. D. Zhang\* and J. I. Budnick

*Department of Physics, University of Connecticut, Storrs, Connecticut 06269  
and Connecticut Advanced Technology Center for Precision Manufacturing and Institute of Materials Science,  
University of Connecticut, Storrs, Connecticut 06269*

D. P. Yang<sup>†</sup> and G. W. Fernando

*Department of Physics, University of Connecticut, Storrs, Connecticut 06269*

W. A. Hines

*Department of Physics, University of Connecticut, Storrs, Connecticut 06269  
and Connecticut Advanced Technology Center for Precision Manufacturing and Institute of Materials Science,  
University of Connecticut, Storrs, Connecticut 06269*

T. D. Xiao

*Connecticut Advanced Technology Center for Precision Manufacturing and Institute of Materials Science,  
University of Connecticut, Storrs, Connecticut 06269*

T. Manzur

*Department of Physics, University of Connecticut, Storrs, Connecticut 06269  
and Connecticut Advanced Technology Center for Precision Manufacturing and Institute of Materials Science,  
University of Connecticut, Storrs, Connecticut 06269*

(Received 16 March 1993; revised manuscript received 15 August 1994)

A calculation of the probabilities for a Y atom having 0, 1, 2, and 3 nearest nitrogen neighbors in the octahedral interstitial ( $9e$ ) sites of the rhombohedral  $Y_2Fe_{17}$  lattice has been carried out according to a continuous solid solution model for the N distribution. In addition,  $^{89}Y$  spin-echo NMR experiments on the  $Y_2Fe_{17}N_x$  system with nominal N content  $0 \leq x \leq 2.8$  were performed in order to compare with the calculated results. The inconsistency between the experimental and calculated results indicates that nitrogen uptake in the  $Y_2Fe_{17}N_x$  system cannot be described by a continuous solid solution model. The NMR results suggest a nitrated/un-nitrated region configuration, i.e., the N atoms absorbed in a  $Y_2Fe_{17}$  sample particle are located in nitrated regions, leaving the remaining part of the particle completely un-nitrated. For the nitrated regions, we find that predominantly only two of the three octahedral interstitial sites around a Y atom are occupied by N atoms. Further nitrogenation produces an increase in the size of the nitrated regions, while the Y-N configuration within these regions does not change during the process if the nitrogenation conditions are kept the same. By using  $^{57}Fe$  NMR, a phase decomposition into YN and  $\alpha$ -Fe precipitates was observed in all of the nitrated samples, including those containing a very small amount of N.

### I. INTRODUCTION

It has been known for a long time that a small amount of C or N can be introduced through diffusion into the bcc  $\alpha$ -Fe lattice.<sup>1</sup> The C and N atoms are located in the octahedral interstitial sites, which are either along the cube edges, half way between the Fe atoms, or at the face centers. The principal effect of these atoms on the magnetic properties of  $\alpha$ -Fe is to cause a magnetic aftereffect

in the magnetic response at low fields.<sup>1</sup> However, completely different results are observed when C, N, or H atoms are diffused into the  $R_2Fe_{17}$  phase, where R is a rare-earth element. The significance of the discovery of  $Sm_2Fe_{17}N_x$  goes far beyond the fabrication of a new permanent magnetic material.<sup>2-5</sup> The improvement in the magnetic properties of all the  $R_2Fe_{17}Z_x$  and  $Nd_2Fe_{14}BZ_x$  compounds,<sup>6</sup> as well as the  $R(Fe,T)_{12}Z_x$  series, in which T is a transition-metal element other than Fe, and  $Z=C$ ,

N or H,<sup>7,8</sup> indicates that this is a general way to modify the magnetic properties of complex multielement magnetic materials or, more generally, the properties of solids in which there are clear interstitial sites available. Perhaps, the magnetic property enhancement effect resulting from gas-phase atomic insertion that is found in the (*R*-Fe)-based binary and ternary systems exists as well in other Fe-based magnetic materials for which the Fe-Fe exchange coupling increases with increasing Fe-Fe distance. Furthermore, similar effects also exist in other Fe alloys.<sup>9</sup> However, unless one has a clear understanding of the interactions which produce the improvement, the gas-atom insertion approach cannot be used to its fullest potential. Therefore, it becomes very important to study the gas-phase modified system on a fundamental basis and on a microscopic scale. One such important issue is the gas atom diffusion process in the 2:17 lattice. Since the improvement of the magnetic properties of the  $R_2Fe_{17}$  nitrides or carbides is produced by the insertion of N or C atoms, the determination of the location and distribution of these atoms in the 2:17 lattice is the basis for further investigations. Although there is some evidence to the contrary,<sup>10,11</sup> it is generally believed that the N and C atoms are located in the octahedral interstitial sites ( $6h$  for hexagonal and  $9e$  for rhombohedral), which are in the basal planes surrounding the *R* atoms.<sup>12-15</sup> This yields the formula unit  $R_2Fe_{17}N_3$  for a completely nitrated ideal structure. Most of the reported  $R_2Fe_{17}$  nitrides or carbides have a N or C content less than three atoms per formula unit, and all of these materials contain some amount of  $\alpha$ -Fe and RN or RC precipitates. In the case that not all of the octahedral interstitial sites are occupied, a detailed picture of the distribution of the N or C atoms in the lattice is needed. For example, a large number of studies deal with the  $R_2Fe_{17}$  nitrides with intermediate N content. Early on, in the studies of  $R_2Fe_{17}N_x$ , it was suggested that the N atoms are distributed homogeneously throughout the entire volume of a particle in the analyses of some experimental results.<sup>16-18</sup> However, the whole picture may change significantly if a preferred N or C distribution profile exists in these systems. The distribution of interstitial atoms is reached through a diffusion process. Therefore, a study of the diffusion of these interstitial atoms will promote our knowledge of the N or C atom distribution, magnetic property improvement and the stability of the magnetic properties. In this regard, there have been several studies.<sup>19-29</sup>

An attempt to deal with the diffusion process of N atoms into the 2:17 lattice was made by Coey, Skomski, and Wirth.<sup>28</sup> They considered the nitrogenation as a simple "free" diffusion of N atoms in the 2:17 lattice, which resulted in a continuous solid solution distribution (CSSD) profile of the N concentration for intermediate N content, and some magnetic properties were explained based on this pattern.<sup>26-29</sup> To date, however, this model has not been tested on a microscopic scale, and some observations, such as the irreversibility of N uptake, are contradictory with it.<sup>29</sup> Moreover, recent experimental results obtained by using optical metallograph and electron microprobe,<sup>20-22</sup> magneto-optical microscopy,<sup>23,25</sup>

and electronic microanalysis techniques<sup>24</sup> were inconsistent with the CSSD pattern. This situation calls for an exploration of the dynamic behavior of N atoms in the 2:17 lattice on a microscopic scale.

It has been observed in the NMR studies of  $Y_2Fe_{17}$  nitrides that the <sup>89</sup>Y resonance frequency is very sensitive to the presence of N atoms as nearest neighbors.<sup>30,31</sup> Therefore, information concerning the distribution of the N atoms in the  $Y_2Fe_{17}$  lattice can be obtained from <sup>89</sup>Y NMR measurements. This paper provides a systematic spin-echo NMR study of the  $Y_2Fe_{17}$  nitrides. A brief discussion on the preconditions required for establishing the CSSD profile and the correlation of such a profile to <sup>89</sup>Y NMR spectra are discussed in Sec. II. In Secs. III-V, we present a test of the feasibility of the CSSD using NMR. Since the experimental results are contradictory to the CSSD model, we propose an alternate model for the N diffusion behavior and distribution pattern in Sec. VI. Finally, the stability of the nitrogen distribution is analyzed based on the model proposed.

## II. CORRELATION OF CONTINUOUS SOLID SOLUTION DISTRIBUTION OF NITROGEN ATOMS AND PROBABILITY FOR NITROGEN ATOMS TO OCCUPY THE OCTAHEDRAL INTERSTITIAL SITES

If a solid sample particle is surrounded by gas atoms and the conditions are suitable for these gas atoms to diffuse in the solid, they migrate into the interior of the particle. The state of the gas-atom system in the particle can be described by its concentration distribution,  $c(x, y, z, t)$ , which is a statistically averaged quantity over a macroscopically small volume [around  $(x, y, z)$ ] and for finite time  $t$ . In a simple approach, the diffusion can be treated by making two basic assumptions. The first is to assume that the development of the system from an inhomogeneous state to the equilibrium state is driven only by the concentration gradient; i.e., no any other interactions are involved. The second is to assume that in a local region, the gas-atom occupation at the available interstitial sites is random and described by the binomial formula. Hereafter, we refer to the diffusion of this gas system as a "free" diffusion process. In the discussion below, we ignore the complexity of the absorption of gas atoms at the particle surface and assume that the gas-phase concentration at the surface is a constant  $c_0$ , and the diffusion is a radial (spherically symmetric) migration process. The diffusion process can be described by Fick's first law

$$J(r, t) = -D \nabla c(r, t) \quad \text{for } r \leq R, \quad (1)$$

where  $J(r, t)$  is the radial flux of the gas atoms across a unit area at a distance  $r$  from the center of the particle,  $c(r, t)$  is the concentration of the gas atoms at  $r$  and a time  $t$ ,  $D$  is the diffusion constant, and  $R$  is the radius of the particle. According to the continuity condition (Fick's second law)

$$\nabla \cdot J(r, t) = -\frac{\partial c(r, t)}{\partial t}, \quad (2)$$

and the diffusion equation can be written as

$$\frac{\partial c(r,t)}{\partial t} = D \nabla^2 c(r,t) \quad \text{for } r \leq R. \quad (3)$$

The initial and boundary conditions are for  $t=0$ ,  $c(r < R, 0) = 0$  and at the surface,  $c(R, 0) = c(R, t) = c_0$ . At an intermediate stage ( $t = \tau$ ) of the diffusion process, the gas-phase concentration distribution is obtained by solving the above diffusion equation<sup>32</sup>

$$c(r, \tau) = c_0 \left[ 1 - \frac{2R}{\pi r} \sum_{m=1}^{\infty} \frac{(-1)^{m+1}}{m} \sin \frac{m\pi r}{R} e^{-m^2 \pi^2 \alpha} \right], \quad (4)$$

where  $\alpha = D\tau/R^2$  is a measure of the approach to the equilibrium distribution through diffusion. Equation (4) demonstrates a continuous solid solution distribution (CSSD) pattern of the gas-phase atoms in the particle during the diffusion process. This is a principal characteristic for a free diffusing gas system. If the process continues for a long time ( $t \gg R^2/D$ ), a uniform gas atom distribution with concentration  $c = c_0$  can be reached.

Another principal characteristic for this system is that if the gas source is terminated at  $t = \tau$ , but the particle remains at the same temperature (and assuming that the gas atoms absorbed in the particle are not released from the particle), these atoms will continue to diffuse toward the interior until an equilibrium gas atom distribution is reached throughout the entire particle. The equilibrium concentration is equal to the average gas atom concentration over the volume of the particle at time  $\tau$ ,  $\bar{c}(\tau)$ , and can be determined by integrating Eq. (4) over the volume of the particle,

$$\bar{c}(\tau) = c_0 \left[ 1 - \frac{6}{\pi^2} \sum_{m=1}^{\infty} \frac{1}{m^2} e^{-m^2 \pi^2 \alpha} \right]. \quad (5)$$

Equations (4) and (5) were used by Skomski and co-workers<sup>26-29</sup> to describe the nitrogen diffusion behavior and related properties of the 2:17 systems. We will now apply the CSSD pattern to the N site occupancy in the  $R_2\text{Fe}_{17}$  system. In order to simplify the discussion, in this work we make the assumption that N atoms occupy only the octahedral interstitial sites.<sup>10,11,14,15</sup> For convenience in the discussion below, we describe the N concentration  $c(r, t)$  as the fraction of N atom occupation in the interstitial sites and hence,  $c_0 = 1$ . In the expression  $R_2\text{Fe}_{17}\text{N}_x$ ,  $x$  is the number of N atoms per  $R_2\text{Fe}_{17}$  formula unit. In the case of an inhomogeneous N concentration distribution,  $x$  represents the average N content. Note that there are three available octahedral interstitial sites per formula unit; therefore,  $x = 3\bar{c}(\tau)$ . Following the above approach, the N occupation in the three octahedral interstitial sites around a Y atom can be determined from the binomial formula, i.e., the probability for a Y atom in a macroscopically small volume near  $r$  to have  $n$  nearest-neighbor N atoms (0, 1, 2, or 3) is

$$P[n, c(r, \tau)] = \frac{3! [1 - c(r, \tau)]^{3-n} c(r, \tau)^n}{n! [3 - n]!}, \quad (6)$$

where  $n = 0, 1, 2$ , and  $3$ , and  $c(r, \tau)$  is expressed by Eq.

(4) with  $c_0 = 1$ . Integrating over the volume of the particle, the probabilities for a  $R$  atom having  $n$  nearest N neighbors for a given average N content  $x$  can be written as

$$P(n, x) = \int_0^R \frac{3! [1 - c(r, \tau)]^{3-n} c(r, \tau)^n}{n! [3 - n]!} \times 4\pi r^2 dr \left/ \left[ \frac{4\pi R^3}{3} \right] \right. \quad (7)$$

Thus, the NMR spectrum for  $R$  atoms can be utilized to probe the N concentration profile in the 2:17 phase.

It has been found in the spin-echo NMR study of the  $\text{Y}_2\text{Fe}_{17}$  nitrides that the  $^{89}\text{Y}$  NMR peak frequencies for a Y atom having 0, 1, 2, and 3 N nearest neighbors are distinct and centered at 42.7, 36.5, 29.3, and 26.5 MHz, respectively,<sup>30</sup> and their intensities are proportional to the probabilities for the Y atom having the corresponding N configurations. Therefore, the  $^{89}\text{Y}$  NMR intensities in the spectrum of  $\text{Y}_2\text{Fe}_{17}\text{N}_x$  can be compared with the probabilities predicted by Eq. (7). In this work, we test the feasibility of the CSSD model for N diffusion in the  $\text{Y}_2\text{Fe}_{17}$  lattice using  $^{89}\text{Y}$  spin-echo NMR by determining (1) whether or not the concentration distribution for the inserted N atoms follows a CSSD pattern in intermediate stages of the nitrogenation process, and (2) whether or not the N distribution profile continues to change under vacuum annealing and ultimately reaches a uniform distribution in a reasonable period of time.

### III. SAMPLE PREPARATION AND THE NMR EXPERIMENT

In order to test the CSSD model, it is necessary to investigate the  $^{89}\text{Y}$  NMR spectra for  $\text{Y}_2\text{Fe}_{17}\text{N}_x$  with intermediate N content. There are several ways to vary the N content in the  $\text{Y}_2\text{Fe}_{17}$  lattice. In order to make the experimental conditions consistent with the requirement of the CSSD model, it is necessary to ensure that the N concentration at the surface of a particle is the same for all of the samples. In this regard, it was decided to vary the N content by preparing samples with different particle sizes and nitriding them under the same conditions. The  $\text{Y}_2\text{Fe}_{17}$  ingots, which were made by arc-melting, were ground to powders which were then passed through sieves to provide six separate samples with particle diameters of <20, 20-25, 25-32, 32-37, 37-43, and >43  $\mu\text{m}$ . The powder samples were wrapped with Ta foils, vacuum sealed in a quartz tube, and then annealed at 950°C for a week prior to nitrogenation. Both x-ray diffraction and NMR were employed to check the phase constituents of the samples. An essentially single phase  $\text{Y}_2\text{Fe}_{17}$  rhombohedral structure, with no  $\alpha$ -Fe present, was identified for all of the powder samples. In order to ensure the same nitrogenation conditions for these samples, they were placed together in the same oven and annealed at 460°C for 17 h under an ultrahigh purity  $\text{N}_2$  (99.999%) gas flow with a pressure of 1 bar. The nitrogen content, namely the average number of N atoms per  $\text{Y}_2\text{Fe}_{17}$  formula unit, was determined by weighing each  $\text{Y}_2\text{Fe}_{17}\text{N}_x$  sample before and after nitrogenation. This re-

sulted in nominal N content values of  $x = 2.8, 2.6, 2.4, 1.8, 1.2,$  and  $0.6$  for the samples with particle diameters of  $< 20, 20-25, 25-32, 32-37, 37-43,$  and  $> 43 \mu\text{m}$ , respectively. Since these samples are nitrogenated under the same conditions, the N concentration at the surface of these samples is the same, thus the difference in their N content reflects the difference in N concentration distribution in these samples.

The  $^{89}\text{Y}$  hyperfine field (HF) distribution measurements were carried out at 4.2 K over a frequency range from 20 to 60 MHz using a phase-coherent spin-echo NMR spectrometer. We refer the reader to Ref. 33 and the references therein for the details of NMR in magnetically ordered materials, instrumentation and experimental procedures.

#### IV. NMR STUDY OF NITROGEN CONCENTRATION DISTRIBUTION IN THE $\text{Y}_2\text{Fe}_{17}\text{N}_x$ LATTICE

Figure 1(a) shows the  $^{89}\text{Y}$  spin-echo NMR spectra for  $\text{Y}_2\text{Fe}_{17}\text{N}_x$  with  $x = 0, 0.6, 1.2, 1.8, 2.4, 2.6,$  and  $2.8$ . As expected, a strong single resonance peak was observed at 42.5 MHz for  $\text{Y}_2\text{Fe}_{17}$  ( $x = 0$ ). For the nitrided samples, four NMR peaks were observed centered at 42.7, 36.5, 29.3, and 26.5 MHz, which were assigned to the Y atoms having 0, 1, 2, and 3 nearest N neighbors, and labeled Y(0), Y(1), Y(2), and Y(3), respectively.<sup>30</sup> For the spectra shown in Fig. 1(a), as the N content increases, the intensity of the Y(0) peak gradually decreases, while the intensities of the Y(1), Y(2), and Y(3) peaks increase. For

$x = 2.8$ , the Y(0) peak essentially disappears, indicating that the particle is almost fully charged with N atoms. The relative intensities of the NMR peaks in each spectrum represent the probabilities of a Y atom having 0, 1, 2, and 3 nearest N neighbors.

In order to compare with the above experimental results, we have computed the overall probabilities [Eq. (7)] for a Y atom having 0, 1, 2, and 3 nearest N neighbors based on the CSSD profile of N distribution for each one of the samples in the  $\text{Y}_2\text{Fe}_{17}\text{N}_x$  series. Assuming that all of the N atoms absorbed by the sample particle enter the 2:17 phase, the average N concentration  $\bar{c}(\tau)$  in Eq. (5) can be evaluated from the measured value of N content per formula  $x$  by  $\bar{c}(\tau) = x/3$ . Subsequently,  $\alpha$  can be determined numerically from Eq. (5) using  $c_0 = 1$ . Inserting the value of  $\alpha$  into Eq. (4),  $c(r, \tau)$  is then calculated numerically for small increments of  $r$  ( $0 \leq r \leq R$ ) for a particular  $\text{Y}_2\text{Fe}_{17}\text{N}_x$  particle. This spatial distribution inside the spherical particle is a continuous one with the largest concentration  $c_0 = 1$  at the surface ( $r = R$ ) and gradually decreasing in concentration towards the center of the particle. Using each numerical value of  $c(r, \tau)$  at a specific location  $r$  in the particle, the local probabilities  $P(0), P(1), P(2),$  and  $P(3)$  are calculated using Eq. (6). The overall probabilities can then be obtained by numerical integration over the entire volume of the particle following Eq. (7). Figure 1(b) shows the computed overall probabilities  $P(0), P(1), P(2),$  and  $P(3)$  for a Y atom having 0, 1, 2, and 3 nearest N neighbors, respectively, for each of the experimentally determined average N con-

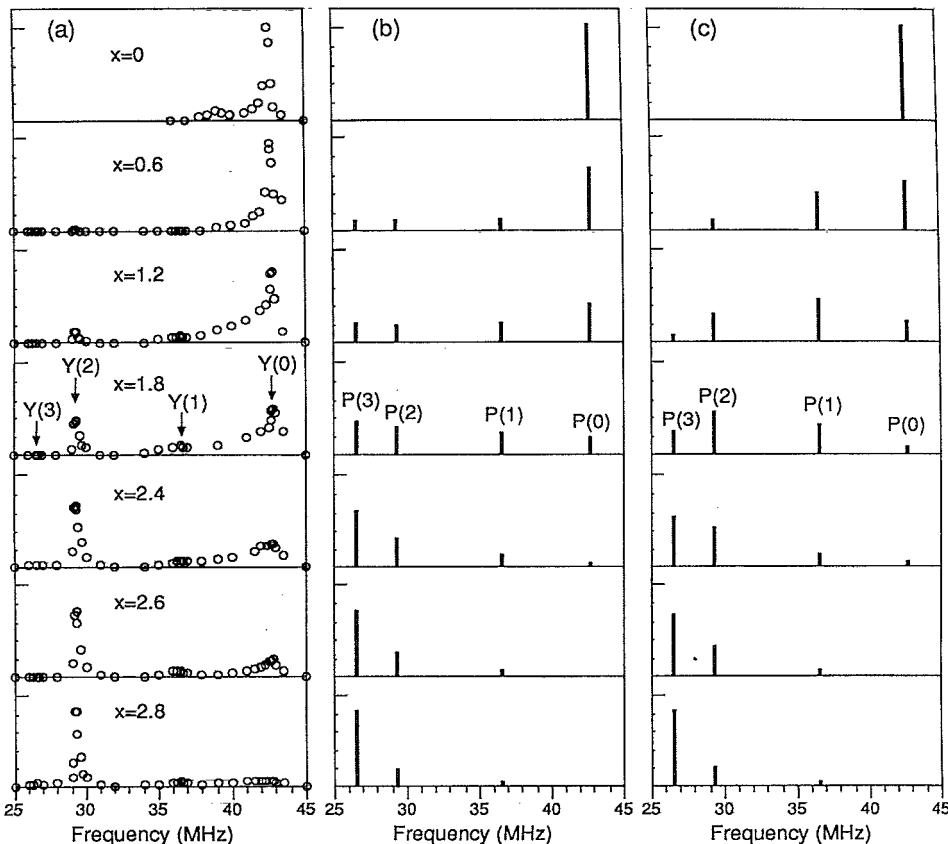


FIG. 1. (a)  $^{89}\text{Y}$  spin-echo NMR spectra for  $\text{Y}_2\text{Fe}_{17}\text{N}_x$  measured at 4.2 K with  $x = 0, 0.6, 1.2, 1.8, 2.4, 2.6,$  and  $2.8$ . Y(0), Y(1), Y(2), and Y(3) represent the resonance peaks for the  $^{89}\text{Y}$  nuclei having 0, 1, 2, and 3 nearest N neighbors, respectively. (b) Computed probabilities for a Y atom having 0, 1, 2, and 3 N nearest neighbors based on Eq. (7) for  $\text{Y}_2\text{Fe}_{17}\text{N}_x$  with  $x = 0, 0.6, 1.2, 1.8, 2.4, 2.6,$  and  $2.8$ . It is assumed in the computation that  $x$  denotes the average N content and that the N concentration distribution profile follows the CSSD pattern [Eq. (4)]. (c) Computed probabilities based on Eq. (6) for the same  $\text{Y}_2\text{Fe}_{17}\text{N}_x$  compositions with  $\bar{c}(\tau) = x/3$  replacing  $c(r, \tau)$ . Here, it is assumed that the N atoms in the lattice are homogeneously distributed throughout a particle.

tents values. It can be seen that the calculated probabilities for the N configuration in the  $Y_2Fe_{17}$  lattice based on the CSSD profile are completely different from the experimentally observed NMR intensities. In particular:

(1) As the N content increases, the CSSD pattern predicts [Fig. 1(b)] a large change in the absolute values of  $P(1)$ ,  $P(2)$ , and  $P(3)$ . For example, with  $x=0.6$ ,  $P(1)$ ,  $P(2)$ , and  $P(3)$  have the values of 0.13, 0.10, and 0.09, respectively; however, with  $x=2.8$ , they have completely different values of 0.02, 0.16, and 0.81. As shown in Fig. 1(a), the relative intensities for the Y(1), Y(2), and Y(3) peaks are approximately the same (about 2:20:1) throughout the entire N content range.

(2) The CSSD pattern predicts [Fig. 1(b)] that  $P(1)$  should be the strongest among  $P(1)$ ,  $P(2)$ , and  $P(3)$  for  $x \leq 1.2$  and  $P(3)$  the strongest for  $x \geq 1.5$ . The NMR spectra [Fig. 1(a)] show that the Y(2) peak has the largest intensity among the Y(1), Y(2), and Y(3) peaks for the entire N content range ( $x \geq 0.6$ ), meaning that in the nitrided regions, most Y atoms have two octahedral N atoms as nearest neighbors. We note that similar results have been reported previously.<sup>10,14,19</sup>

(3) The Y(3) peak intensity is much weaker than expected based on the computed  $P(3)$ , and is the weakest peak for the entire N content range. Especially for  $x=2.8$ ,  $P(3)=0.81$  according to the CSSD model [Fig. 1(b)], while the actual probability (absolute fraction of the  $^{89}Y$  intensity) measured from the NMR experiment is only 0.04, a 20-fold discrepancy.

(4) The major change in the spectra shown in Fig. 1(a) lies in the decrease of the Y(0) peak intensity with respect to the Y(1), Y(2), and Y(3) peaks, which have a relatively constant ratio. However, as shown in Fig. 1(b), the CSSD model predicts that the decrease in  $P(0)$  results in an increase of  $P(1)$ ,  $P(2)$ , and  $P(3)$  in a different manner. Specifically, for increasing  $x$  with  $x \leq 1.2$ ,  $P(1)$ ,  $P(2)$ , and  $P(3)$  have roughly an even growth; however, for  $x \geq 2.2$ ,  $P(3)$  increases drastically while  $P(1)$  and  $P(2)$  decrease.

The inconsistencies between the computed probabilities for these Y-N configurations based on the CSSD profile and the experimental NMR peak intensities are large; and the existence of these inconsistencies over a wide range of N content indicates that such inconsistencies occur not just in the defect regions, but essentially throughout the entire volume of the particle. Therefore, we conclude that the CSSD model is not a suitable description for the nitrogen distribution in the  $Y_2Fe_{17}$  lattice.

#### V. EXPLORATION OF THE STABILITY OF NITROGEN DISTRIBUTION PROFILE UPON VACUUM ANNEALING

For a free diffusing gas atom system, when the gas source is cut off after nitriding for a certain period of time but with the temperature remaining the same, two situations are possible. (1) The N atoms which entered the lattice will leave the particle. (2) In the case where there is a surface barrier, the diffusion process will continue for the atoms inside the particle until the gas-phase

atoms reach a uniform concentration distribution throughout the particle. In the former case,  $P(0)$  will drastically increase, while  $P(1)$ ,  $P(2)$ , and  $P(3)$  will decrease and eventually disappear. In the latter case,  $P(0)$ ,  $P(1)$ ,  $P(2)$ , and  $P(3)$  can be easily calculated using Eqs. (6) by inserting the value of  $\bar{c}(\tau)$  in place of  $c(r, \tau)$ . Figure 1(c) shows the calculated probabilities for a Y atom having 0, 1, 2, and 3 nearest N neighbors for a uniform N concentration distribution for each of the samples, assuming that the vacuum annealing does not result in N outgassing from the samples. To test the behavior of the N atoms, the  $Y_2Fe_{17}N_{1.8}$  sample was sealed in a quartz tube under vacuum and annealed at 460°C for 3 days. The volume of the tube was sufficient for evacuating most N atoms from the sample. The NMR spectrum of the annealed sample was then remeasured. Figure 2 shows a comparison of the NMR spectra measured from the  $Y_2Fe_{17}N_{1.8}$  before and after vacuum annealing. The difference in character for the N atoms in the  $Y_2Fe_{17}$  lattice from that predicted by the CSSD model is evident.

For the as-nitrogenated  $Y_2Fe_{17}N_{1.8}$  sample, the measured intensity ratio Y(0):Y(1):Y(2):Y(3) is 26:2:21:1; while the computed probabilities  $P(0)$ ,  $P(1)$ ,  $P(2)$ , and  $P(3)$  for a homogeneous N distribution [Eq. (6)] are 0.06, 0.29, 0.43, and 0.22, respectively, which correspond to an intensity ratio of 3:14:21:11. If a free diffusion process took place for the N atoms in this  $Y_2Fe_{17}N_{1.8}$  sample, 3 days would have been long enough for these atoms to reach a homogeneous distribution and, consequently, we would observe a large change in the NMR spectrum after annealing. As shown in Figs. 2(a) and 2(b), however, there is no change in the (relative) intensity ratio of the

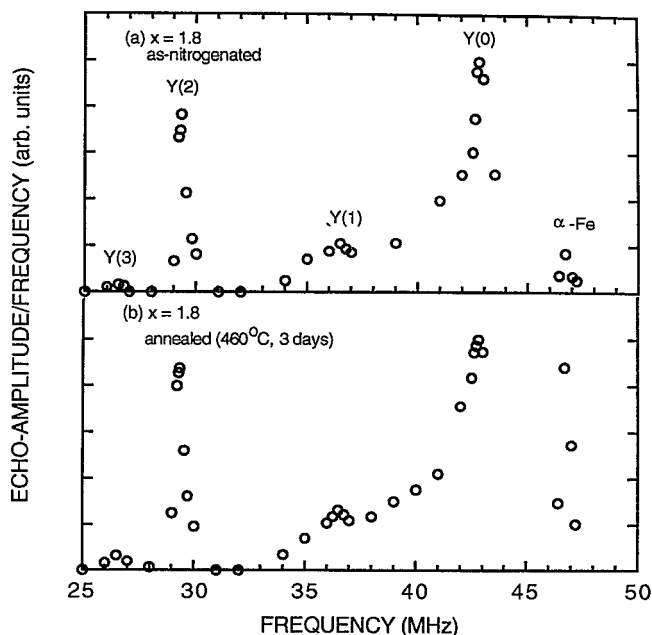


FIG. 2.  $^{89}Y$  spin-echo NMR spectra for  $Y_2Fe_{17}N_{1.8}$ : (a) as-nitrogenated, and (b) annealed at 460°C in vacuum for 3 days. Vacuum annealing for a long time does not result in a redistribution of the N atoms which entered the octahedral sites, although there is an increase in phase precipitation ( $\alpha$ -Fe).

Y(1):Y(2):Y(3) peaks or in the intensity ratio of these peaks relative to the Y(0) peak. The only observable change in the NMR spectrum for the  $Y_2Fe_{17}N_{1.8}$  sample is due to an increase in phase precipitation as indicated by the increase in intensity of the  $\alpha$ -Fe peak. In addition, the  $Y_2Fe_{17}N_{2.8}$  sample was annealed at 490°C for 5 h and the  $^{89}Y$  NMR spectrum was remeasured. Again, no change in the spectrum was observed.

These results demonstrate that, upon further annealing at temperatures equal or even higher than that previously used for nitrogenation, the N atoms which have been absorbed into the octahedral interstitial sites of the  $Y_2Fe_{17}$  lattice neither leave the lattice nor redistribute on a macroscopic scale and reach a homogeneous distribution state.

## VI. DISCUSSION

### A. N diffusion and distribution

Based on the NMR results, we have proposed the following model for the N distribution.<sup>34</sup> The  $Y_2Fe_{17}N_x$  compound with intermediate N content is separated spatially into a nitrided phase, in which two out of the three interstitial sites are occupied by N atoms (see the next subsection for details), and an unnitrided  $Y_2Fe_{17}$  phase. The nitrogen content  $x$  reflects the relative volume of the nitrided regions. The Y(2) and Y(3) NMR peaks originate from the Y atoms in the nitrided regions, while the Y(0) peak comes mainly from the Y atoms in the unnitrided regions. Between the two regions in a particle, there exists a boundary region where the Y atoms mostly have 1 N atom as a nearest neighbor, which leads to the appearance of the Y(1) peak. According to this model,

the nitrogenation process is the volume growth of the nitrided regions, while the Y-N configuration within it is unchanged during the process if the nitrogenation conditions remain the same. The disappearance of the Y(0) peak is an indication of the completion of nitrogenation. In order to show the difference between the two-phase configuration model and the CSSD model, the nitrogen concentration distribution profiles for the  $Y_2Fe_{17}N_x$  samples are sketched following the two phase configuration idea in Fig. 3(a), and compared with those predicted by the CSSD model with inhomogeneous distributions [Fig. 3(b)] and equilibrium distributions [Fig. 3(c)]. In drawing Fig. 3(a), it is assumed that the two-phase has an outer-shell/inner-core steric structure. However, as pointed out in Ref. 20, the nitrogen diffusion may not necessarily originate through the particle surface, but perhaps more easily through the defects (cracks). This makes the nitrided/unnitrided configuration different from an ideal outer-shell/inner-core structure. The complexity concerning the detailed construction of the nitrided regions does not affect the validity of the two-phase model. In addition to the present NMR experiments, several other experimental observations concerning the N distribution in the  $R_2Fe_{17}$  nitrides<sup>20-24</sup> and  $R_2Fe_{14}B$  nitrides<sup>25</sup> are consistent with our nitrided/unnitrided configuration model. We would like to mention that such a nonrandom N distribution in the  $Y_2Fe_{17}$  system is not something new, similar nonrandom distribution of gas-phase atoms in solids has been observed in many materials.<sup>35,36</sup>

The present NMR experiments show that (1) the N distribution profile formed by nitriding  $Y_2Fe_{17}$  for a certain period ( $\tau$ ) does not follow a CSSD model, (2) this profile does not vary toward a homogeneous distribution during annealing, and (3) the above two features do not just

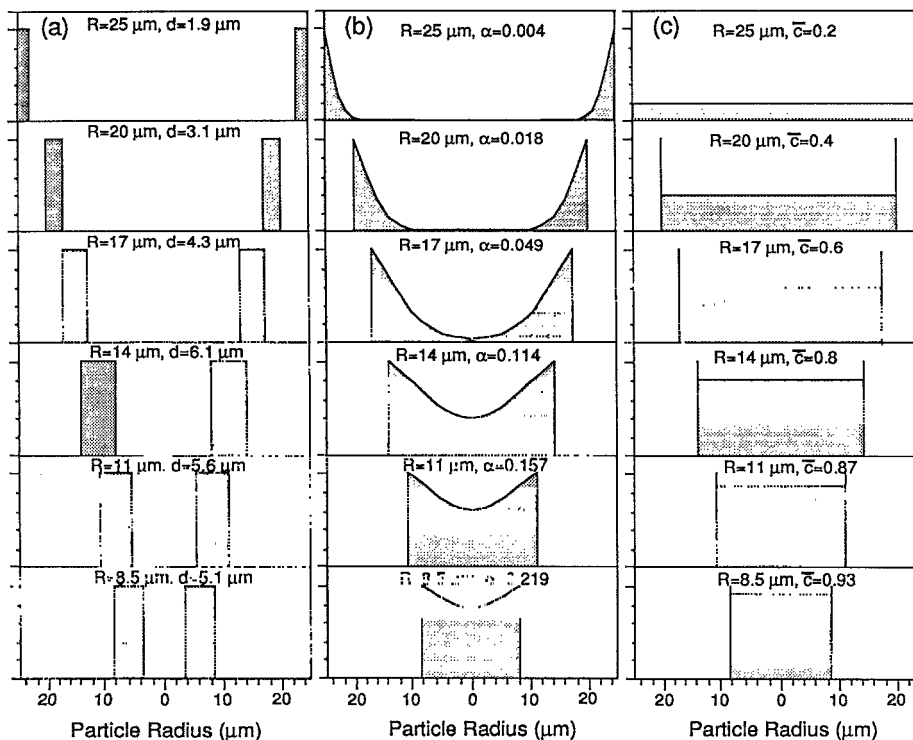


FIG. 3. N concentration distribution profiles in the  $Y_2Fe_{17}$  lattice for sample particles with average radii  $R = 25, 20, 17, 14, 11,$  and  $8.5 \mu\text{m}$ , which corresponds to  $Y_2Fe_{17}N_x$  with N content  $x = 0.6, 1.2, 1.8, 2.4, 2.6,$  and  $2.8$ , respectively. (a) Two phase (nitrided and unnitrided) configuration model, where  $d$  is the thickness of the outer shell (nitrided region). (b) CSSD model with inhomogeneous N concentration distributions [Eq. (4)], where  $\alpha$  is the parameter in Eq. (4). (c) CSSD model with homogeneous N concentration distributions [Eq. (5)], where  $\bar{c}(\tau) = x/3$  is the average N content in equilibrium. Note that the computed probabilities shown in Figs. 1(b) and 1(c) are based on the N concentration distribution profiles shown here in (b) and (c), respectively.

occur in the early diffusion stage (within which the regions around cracks are involved), they are essentially the features of the bulk diffusion. Therefore, it is evident that nitrogenation is not a free N diffusion process. Thus, Eqs. (1)–(3) may not be applicable in their present form in this case. Originally, the driving force for atomic migration is the gradient of chemical potential  $\mu$  and thus,

$$J(r) = D \nabla \mu . \quad (8)$$

Under the assumption that there are no other driving forces involved other than the concentration gradient,  $\mu$  is then a function of N concentration alone and, thus, Eq. (1) is applicable. If there are no traps or barriers that will hinder the migration of a nitrogen atom undergoing diffusion, the continuity condition [Eq. (2)] is satisfied and the nitrogenation can be treated as a free N diffusion process. In this case Eq. (3) is a suitable description of diffusion process, and Eqs. (4) and (5) provide a correct picture of N concentration distribution in the particle. The deviation of the N distribution from the pattern predicted by the CSSD model implies the existence of some significant interaction affecting the nitrogen uptake. One possible factor is a trapping effect similar to that found in a chemical reaction diffusion process which makes the gas-phase atom distribution profile very different from a CSSD pattern.<sup>32,35,36</sup> Another possible factor is the N-N interaction via lattice strain, such as that observed in some metal-hydrogen systems where a nonrandom distribution of H atoms in the metal lattice results from the H-H interaction mediated by elastic coupling of the lattice.<sup>37,38</sup> Further investigation is needed to understand the origin of the nitrated/unnitrided configuration.

#### B. Y-N configuration in the nitrated region of the $Y_2Fe_{17}$ lattice

From the point of view of a basic study, the R-N coordination is a more meaningful parameter than the average N content. Up to now, this issue has not been studied carefully on an atomic scale; in the literature, information concerning the R-N configuration has been obtained from measurements of the nominal N content by gravimetric or volumetric techniques. These measurements include everything gained during nitrogenation process, such as the N in the YN precipitates, N in the particle surface (physical adsorption) or in the bulk, but not at the octahedral sites and, possibly, other impurity atoms. Thus, the actual N content in the 2:17 phase may be significantly less than that measured gravimetrically. Moreover, the distribution of these N in the lattice is not homogeneous. Considering all of these factors, one cannot obtain reliable R-N coordination information from these macroscopic measurements. One of the advantages of NMR is that it directly measures the R-N coordination. Figure 1 shows that, in a nitrated region of a  $Y_2Fe_{17}N_x$  particle, most probably only two of the three octahedral interstitial sites surrounding a Y atom are actually occupied by N atoms; the complete filling of the three octahedral sites by 3 N is much smaller than predicted by the CSSD model. Similar results were reported in some neutron-diffraction (ND) studies.<sup>10,11</sup> One possi-

ble cause for a reduced 3 N occupancy is lattice strain. The CSSD model assumes that the occupation of N atoms in the interstitial sites is random and follows the binomial expression; that is, the probability of having a N site occupied around an Y atom is independent of the nearest N neighbors that are already present. However, the strain produced by N insertion may change the whole picture. The filling of the first octahedral site in the hexagon surrounding a Y atom by a N atom makes the neighboring Fe(12j) atoms move outward, which affects further occupation of N atoms. The distortion of the hexagon due to 2 N filling may severely reduce or even prevent the occupancy of the third interstitial site if the reaction energy for this filling becomes positive.

#### C. Structural stability of the $Y_2Fe_{17}$ nitrides

For gas-atom insertion processing, the distribution stability of the inserted atoms in the 2:17 phase is one of the most important issues, since it is intimately related to the stability of material properties and, consequently, the practical applicability of the material. Among the presently used species in gas-atom modification of  $R_2Fe_{17}$ , C or N uptake is irreversible, while H uptake has been found to be reversible. Therefore, C and N insertion can be employed satisfactorily. The stability of the magnetic properties of  $R_2Fe_{17}N_x$  compounds is related to two factors: (1) the distribution stability of interstitial atoms in the lattice, and (2) the structural stability of the 2:17 phase. In order to avoid phase decomposition, nitrogenation is normally performed at a low temperature. In this case, the 2:17 particles may not be fully nitrated, especially when there exists a rather wide particle size distribution. As the distribution of the inserted N atoms within a particle can be very inhomogeneous [Fig. 3(a)], a question arises as to whether or not the distribution pattern is stable. The  $^{89}Y$  NMR results shown in Fig. 2 have already demonstrated the distribution stability of these N atoms at the nitrogenation temperature. Since the relaxation time for diffusion increases exponentially with decreasing temperature, it can be concluded that the N atoms located in the octahedral interstitial sites will not relocate at room temperature.

However, phase decomposition is a problem. Almost all the  $R_2Fe_{17}$  nitrides or carbides reported in the literature contain some amount of  $\alpha$ -Fe which is a negative factor for permanent magnetic properties. A quantitative estimate of the  $\alpha$ -Fe content in the various  $Y_2Fe_{17}N_x$  was obtained from the spin-echo NMR spectra.  $^{57}Fe$  in  $\alpha$ -Fe is characterized by a sharp peak at 46.7 MHz (e.g., see Fig. 2). As shown in Fig. 4, a monotonic increase of the  $\alpha$ -Fe phase precipitates with N content  $x$  has been observed for the as-nitrogenated  $Y_2Fe_{17}N_x$  samples. For the almost fully nitrated  $Y_2Fe_{17}N_{2.8}$  sample, approximately 6 at. % of the total number of Fe atoms in the sample is in the  $\alpha$ -Fe phase and 94 at. % are in the 2:17 phase. Our experiments on a number of  $Y_2Fe_{17}N_x$  samples show that phase decomposition depends on the nitrogenation conditions. For example, nitrogenation at a higher temperature for a shorter time results in more  $\alpha$ -Fe precipitates for the same N content. In all of the cases

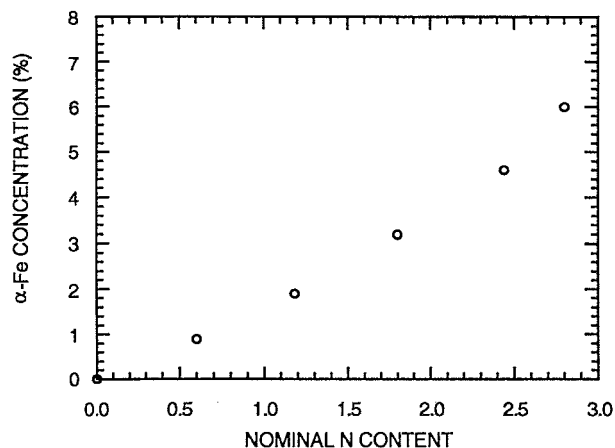


FIG. 4. Bcc  $\alpha$ -Fe content (in at. %) as a function of nominal N content  $x$  for the  $Y_2Fe_{17}N_x$  samples nitrogenated at 460°C for 17 h.

studied, the  $\alpha$ -Fe content increased monotonically with N content for the same nitrogenation conditions. The fact that the parent  $Y_2Fe_{17}$  compound can be made as a pure single phase, while phase decomposition takes place as soon as it starts to absorb N atoms implies that the decomposition is not likely to be due to processing imperfections. It is also worth mentioning that both N and C insertion, which results in a relatively large lattice expansion, produces phase decomposition, while H insertion, which results in a small expansion, does not. This implies that the excess strain produced due to N insertion is one of the causes of phase decomposition in the  $Y_2Fe_{17}$  phase. At this point, the small intensity for the Y(3) peak (compared with that expected for a random occupation of N atoms in these sites) and the occurrence of  $\alpha$ -Fe may be closely related when one considers the decomposition of the  $Y_2Fe_{17}$  nitrides. When the strain produced by the N occupancy in the hexagon exceeds a certain limit, phase decomposition may take place during the nitrogenation process, or afterwards at room temperature. We have observed an aging effect in a  $Y_2Fe_{17}N_{2.6}$  sample by using NMR. Comparing the  $^{89}Y$  NMR spectrum measured right after nitrogenation and the spectrum measured on the same sample after 6 months showed a reduction of the intensity for the Y(3) peak and a significant increase in  $\alpha$ -Fe peak.

Finally, we note that  $\alpha$ -Fe was found in all nitrogenated samples, including the one with  $x=0.6$ . This is consistent with the two-phase N distribution model proposed

here in that the N atoms are concentrated in small nitrided regions. Otherwise, it would be difficult to understand the occurrence of decomposition if such a small amount of N was randomly distributed in a rather large volume.

## VII. CONCLUSIONS

We have carried out a study of N diffusion in the  $Y_2Fe_{17}$  lattice and the relevant structural properties of the nitrides using  $^{89}Y$  and  $^{57}Fe$  spin-echo NMR. A comparison of the experimental results is made with a continuous solid solution distribution (CSSD) model. The results of the study are as follows.

(1) The diffusion of N in the  $Y_2Fe_{17}$  lattice is not a free (or normal) diffusion process.

(2) For the  $Y_2Fe_{17}$  nitrides with intermediate N content, the distribution of N does not follow the CSSD pattern; instead, a particle consists of nitrided and unnitrided regions. The NMR results suggest that in the nitrided regions, predominantly only two of the three possible octahedral interstitial sites around a Y atom are occupied by N atoms.

(3) The distribution for the N atoms which enter the octahedral interstitial sites is stable, but phase decomposition into YN and  $\alpha$ -Fe precipitates increases monotonically with the N content.

Although previous phenomenological treatments<sup>25-28</sup> are a good starting point, a more complete treatment of the N atoms is needed to gain a better understanding of the nitrogenation process in the  $R_2Fe_{17}$  lattice. Some interactions should be introduced in the diffusion equations. In addition to the phenomenological treatment, a microscopic understanding of the nature of the interaction of the N atoms with the 2:17 lattice is very much needed. It will be worthwhile and interesting to calculate the energetics associated with the R-Fe-N system and related phase stabilities with respect to N content. The elastic coupling between the N atoms in the octahedral sites and the binding energies associated with Y and nearest N neighbors would be quite helpful in obtaining a clear picture.

## ACKNOWLEDGMENTS

This work was supported in part by NSF Grant No. DMR9319367 and by Grant No. 91HO14 from the Connecticut Department of Economic Development and the Connecticut Advanced Center for Precision Manufacturing. The authors also thank T. W. Capehart, D. M. Pease, and P. Panissod for useful discussions of the manuscript.

\*Permanent address: Department of Physics, Lanzhou University, Lanzhou, Gansu 730000, P. R. China.

†Permanent address: Department of Physics, College of the Holy Cross, Worcester, MA 01610.

<sup>1</sup>S. Chikazumi, *Physics of Magnetism* (Wiley, New York, 1964), p. 303.

<sup>2</sup>J. M. D. Coey and H. Sun, *J. Magn. Magn. Mater.* **87**, L251

(1990).

<sup>3</sup>K. H. J. Buschow, R. Coehoorn, D. B. de Waard, and T. H. Jacobs, *J. Magn. Magn. Mater.* **92**, L35 (1990).

<sup>4</sup>H. Sun, J. M. D. Coey, Y. Otabi, and D. P. F. Hurley, *J. Phys. Condens. Matter* **2**, 6465 (1990).

<sup>5</sup>X. C. Kou, R. Grossinger, M. Katter, J. Wecker, L. Schultz, H. T. Jacobs, and K. H. J. Buschow, *J. Appl. Phys.* **70**, 2272

- (1991).
- <sup>6</sup>Y. C. Yang, X. D. Zhang, L. S. Kong, Q. Pan, Y. T. Hou, S. Huang, and L. Yang, *J. Less-Common Met.* **170**, 37 (1991).
- <sup>7</sup>D. P. F. Hurley and J. M. D. Coey, *J. Phys. Condens. Matter* **4**, 5573 (1992).
- <sup>8</sup>Y. C. Yang, X. D. Zhang, S. L. Ge, Q. Pan, L. S. Kong, H. Li, J. L. Yang, B. S. Zhang, Y. F. Ding, and C. T. Ye, *J. Appl. Phys.* **70**, 6001 (1991).
- <sup>9</sup>Y. Xu, J. M. Elbicki, W. E. Wallace, S. Simizu, and S. G. Sankar, *IEEE Trans. Magn.* **28**, 2569 (1992).
- <sup>10</sup>S. S. Jaswal, W. B. Yelon, G. C. Hadjipanayis, Y. Z. Wang, and D. J. Sellmyer, *Phys. Rev. Lett.* **67**, 644 (1991).
- <sup>11</sup>W. B. Yelon and G. C. Hadjipanayis, *IEEE Trans. Magn.* **28**, 2316 (1992).
- <sup>12</sup>O. Isnard, S. Miraglia, J. L. Soubeyroux, and D. Fruchart, *J. Less-Common. Met.* **162**, 273 (1990).
- <sup>13</sup>R. M. Ibberson, O. Moze, T. H. Jacobs, and K. H. J. Buschow, *J. Phys. Condens. Matter* **3**, 1219 (1991).
- <sup>14</sup>O. Isnard, S. Miraglia, J. L. Soubeyroux, D. Fruchart, and J. Pannetier, *Phys. Rev. B* **45**, 2920 (1992).
- <sup>15</sup>T. W. Chapehart, R. K. Mishra, and F. E. Pinkerton, *Appl. Phys. Lett.* **58**, 1395 (1991).
- <sup>16</sup>M. Katter, J. Wecker, C. Kuhrt, L. Schultz, and R. Grossinger, *J. Magn. Magn. Mater.* **117**, 419 (1992).
- <sup>17</sup>M. Rosenberg, R. J. Zhou, M. Katter, L. Schultz, and Filoti, *J. Appl. Phys.* **73**, 6035 (1993).
- <sup>18</sup>R. J. Zhou, M. Rosenberg, M. Katter, and L. Schultz, *J. Magn. Magn. Mater.* **118**, 110 (1993).
- <sup>19</sup>J. M. D. Coey and D. P. F. Hurley, *J. Magn. Magn. Mater.* **104-107**, 1098 (1992).
- <sup>20</sup>C. C. Colucci, S. Gama, L. C. Labaki, and A. Ribeiro, *J. Magn. Magn. Mater.* **125**, 161 (1993).
- <sup>21</sup>C. C. Colucci, S. Gama, and F. A. O. Cabral, *IEEE Trans. Magn.* **28**, 2578 (1992).
- <sup>22</sup>C. C. Colucci, S. Gama, and C. A. Ribeiro, *J. Alloys Compounds* **194**, 181 (1993).
- <sup>23</sup>T. Mukai and T. Fujimoto, *J. Magn. Magn. Mater.* **103**, 165 (1992).
- <sup>24</sup>C. C. Colucci, S. Gama, C. A. Ribeiro, and L. P. Cardoso, *J. Appl. Phys.* **75**, 6003 (1994).
- <sup>25</sup>C. Onneby, T. Debroy, and S. Seetharaman, *J. Magn. Magn. Mater.* **127**, 307 (1993).
- <sup>26</sup>R. Skomski and J. M. D. Coey, *J. Appl. Phys.* **73**, 7602 (1993).
- <sup>27</sup>R. Skomski, C. Murray, S. Brennan, and J. M. D. Coey, *J. Appl. Phys.* **73**, 6940 (1993).
- <sup>28</sup>J. M. D. Coey, R. Skomski, and S. Wirth, *IEEE Trans. Magn.* **28**, 2332 (1992).
- <sup>29</sup>J. M. D. Coey, J. F. Lawler, H. Sun, and J. E. M. Allan, *J. Appl. Phys.* **69**, 3007 (1991).
- <sup>30</sup>Cz. Kapusta, M. Rosenberg, J. Zukrowski, H. Figiel, T. H. Jacobs, and K. H. J. Buschow, *J. Less-Common Met.* **172**, 101 (1991).
- <sup>31</sup>Cz. Kapusta, M. Rosenberg, K. Erdmann, and K. H. J. Buschow, *Solid State Commun.* **75**, 121 (1990).
- <sup>32</sup>J. Crank, *The Mathematics of Diffusion* (Oxford University Press, Oxford, 1979), p. 91.
- <sup>33</sup>Y. D. Zhang, J. I. Budnick, J. C. Ford, and W. A. Hines, *J. Magn. Magn. Mater.* **100**, 13 (1991).
- <sup>34</sup>Y. D. Zhang, J. I. Budnick, T. Manzur, and T. D. Xiao, *Bull. Am. Phys. Soc.* **38**, 816 (1993).
- <sup>35</sup>J. Crank, *The Mathematics of Diffusion* (Ref. 32), pp. 286 and 326.
- <sup>36</sup>S. Mrowec, *Defects and Diffusion in Solids* (Elsevier Science, New York, 1980), pp. 217 and 282.
- <sup>37</sup>J. D. Fast, *Interaction of Metals and Gases* (Academic, New York, 1965), p. 183.
- <sup>38</sup>H. Wagner and H. Horner, *Adv. Phys.* **23**, 587 (1974).